

Compact microwave multilayer dual-band bandpass filter with folded dual-mode resonators

A. M. PLAZINIĆ^a, M. M. POTREBIĆ^{b*}, D. V. TOŠIĆ^b

^aPh.D. student, Faculty of Technical Sciences Čačak, University of Kragujevac, 32000 Čačak, Serbia

^bSchool of Electrical Engineering, University of Belgrade, P.O. Box 35-54, 11120 Belgrade, Serbia

This paper presents a novel realization of a multilayer dual-mode resonator. The halves of the folded resonator are printed on the outer sides of the two dielectric layers. A novel dual-band bandpass filter is implemented as a parallel connection of two multilayer dual-mode filters. We are motivated to use this design approach in order to achieve independent tuning of each filter pass band and to minimize the footprint. In order to reduce the simulation time for the filter design, we propose a novel procedure based on the circuit models. The procedure is exemplified by designing a multilayer dual-band bandpass filter and validated by measurements.

(Received November 12, 2016; accepted June 7, 2017)

Keywords: Bandpass filter, Circuit model, Dual-band bandpass filter, Dual-mode resonator, Miniaturization, Multilayer technology

1. Introduction

Due to the increased number of new services and development of new wireless technologies, it is necessary to strictly limit the assigned frequency band for each device. Also, the need for size reduction of the user devices imposes the need to significantly miniaturize the components of wireless systems [1]. The previously mentioned facts, such as the importance of wireless communications, frequency range occupation and miniaturization requirements, point out the particular significance of microwave multi-bandpass filters design such as dual-band bandpass filters design [2-4]. For some applications where the size reduction is of primary importance, smaller planar filters are desirable.

There is an increasing interest in multilayer filters to meet the size, performance and cost requirements. Multilayer technology also provides another dimension in the flexible design and integration of other microwave components, circuits and subsystems. In order to accomplish the requirements, it is necessary to investigate possibilities for implementing filters to meet specification requirements such as filter type, centre frequency, bandwidth, insertion loss, return loss, unwanted band suppression, selectivity and footprint.

Particular implementation of the filter elements depends on the chosen technology. If the planar technology is used there are various approaches for filter implementation as microstrip filters with dual-mode capacitively loaded resonator [5], microstrip stepped impedance resonator (SIR) filters [4], split rings resonators [6], quasi-dual-mode resonator [7], multilayer filters with apertures on the common ground plane [8], filter with reduced-length parallel coupled lines [9] and multilayer resonator using double-sided microstrip [10]. For the above mentioned filter design examples, a common approach is to find relations between geometrical characteristics of the

element implementations and the corresponding element values. These relations are typically generated by extensive 3D EM simulations.

Dual-mode resonators have often been used for dual-band bandpass filter design, as in [11-14]. Dual-mode resonators have been widely used to realize many RF/microwave filters [1, 15-16]. A main feature and advantage of this type of resonators lies in the fact that each of dual-mode resonators can be used as a doubly tuned resonant circuit, and therefore the number of resonators required for an n -degree filter is reduced by one-half, resulting a compact filter configuration [1].

In this paper, we propose a novel compact resonator using a double-sided microstrip with the common ground in between. With this type of implementation in multilayer technology, component layout is no longer confined to one plane so that leaves a greater degree of freedom in allocating individual components. In addition, we design a microwave dual-band bandpass filter with multilayer dual-mode resonators. The structure is realized as a parallel connection of two multilayer dual-mode filters. Our goal is to design a dual-band bandpass filter whereby one resonator for each of the bands is used. Each of the resonators is configured according to the requirements of the appropriate band. The main requirement of the research is that the resonators from neighbouring bands are not mutually coupled. Each of the bands can be adjusted independently in the realization of the multi-band filter as in [17].

We use 3D EM simulator WIPL-D [18] for the design and analysis of the considered structures. Besides the 3D EM models, in this paper, we propose circuit models for filter design. The concept of the circuit model is used as a primary tool for filter design and analysis. The circuit-level simulators analyze the filter almost instantaneously and we use these simulations to find how filter elements affect its characteristics [19]. The 3D filter structure has

been decomposed into domains and each of them is modelled by a microwave network. After fine tuning, these filters are analyzed by 3D EM solvers. The 3D EM model is validated by measurements on the fabricated filter.

We are motivated to propose this design methodology because we want to achieve independent control and tuning of the pass bands of each filter, which implies independent tuning of the corresponding resonators. Our additional motivation is to achieve compact filter design with a smaller footprint.

2. Filter design with dual-mode resonator

One approach to the realization of a compact filter is to use dual-mode resonators. In this paper, we used the resonator with the short circuited centre stub. It is easy to adjust specified filter selectivity by using these resonators.

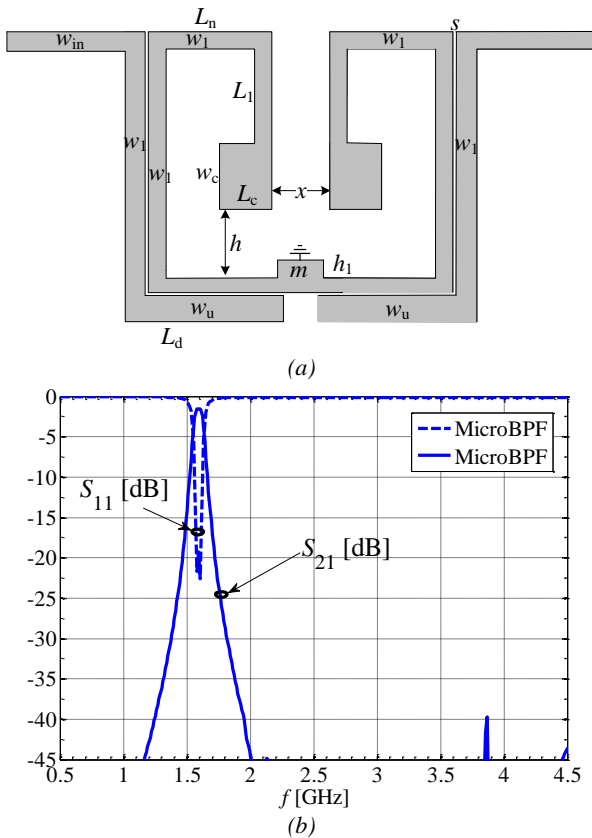


Fig. 1. a) 3D EM model of the microstrip filter with dual-mode resonator, b) S-parameters of the filter with dual-mode resonator, obtained by simulation

The filter is implemented in microstrip technology. The resonator is capacitively coupled to the feed lines implemented as a 50Ω microstrip line ($w_{in} = 1.1$ mm). The filter is designed for the centre frequency of 1.6 GHz (f_0) and a fractional bandwidth (FBW) of about 5.56%. In this study, we use laminate TLE-95-0200-CH/CH, with the following parameters: $\epsilon_r = 2.95$, $\tan\delta = 0.001$, substrate thickness $h = 0.508$ mm, metallization thickness $t = 18 \mu\text{m}$. The conductor conductivity is set to $\sigma = 20$ MS/m to take

into account the losses due to the surface roughness and the skin effect.

Table 1. Parameters of the filter with dual-mode resonator (MicroBPF) shown in Fig. 1a. All dimensions are in mm

w_1	s	L_n	L_d	w_c	L_c
1.1	0.1	5.1	6.28	2.7	2.85
x	w_u	m	h_1	h	L_1
2.1	1.4	1.8	0.9	4.3	3.8

3D EM model of the microstrip bandpass filter (MicroBPF) is shown in Fig. 1a and the filter dimensions are given in Table 1. S-parameters of the filter, obtained by simulation, are shown in Fig. 1b.

3. Multilayer filter design with dual-mode resonator

In this section, we propose miniaturization of the filter designed with a dual-mode resonator as shown in Fig. 1a. The microstrip filter is symmetric with respect to the axis of symmetry. Miniaturization is obtained by folding the resonator in two layers along the axis of symmetry.

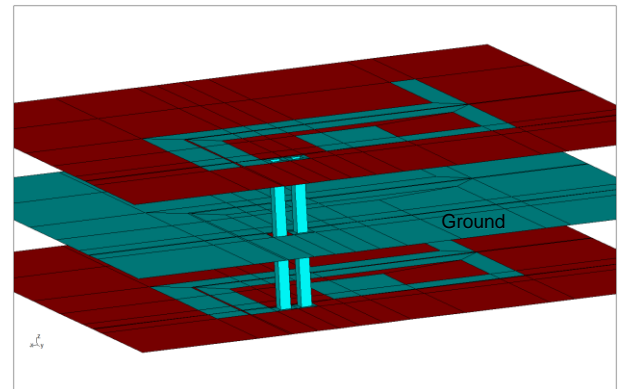


Fig. 2. Filter miniaturization in multilayer technology

The structure consists of two dielectric layers, which are separated by a conducting plane - the common ground, Fig. 2. The halves of the resonator are printed one below the other, on different sides of the dielectric layers.

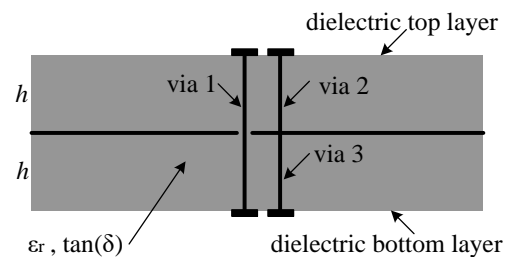


Fig. 3. Vias in cross section of the filter: via 1 connects parts of the resonator, vias 2 and 3 connect resonator with the common ground plane

Electrical connection between the halves of the resonator, printed on opposite sides of the structure, is realized by using vias, as shown in Fig. 3. The via 1 is used to connect parts of the resonator without electrical contact with the common ground plane. This is achieved by removing the common ground around the via 1 in the central plane of the structure. Two vias 2 and 3 are used for grounding the miniaturized resonator as shown in Fig. 3. These vias connect the common ground with the top and bottom parts of the resonator.

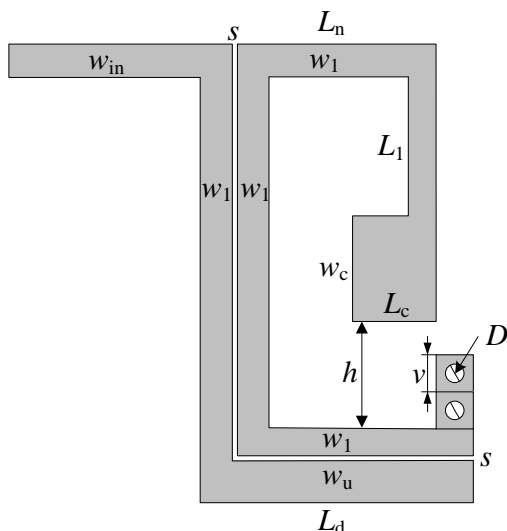


Fig. 4. 3D EM model of MultiBPF-1B for the centre frequency of 1.6 GHz

Table 2. Parameters of the MultiBPF-1B shown in Fig. 4. All dimensions are in mm

w_1	s	D	w_c	h	v
1.1	0.1	0.5	2.7	4.3	1.0
L_1	w_u	L_d	L_c	L_n	
3.8	1.4	6.28	2.85	5.1	

The multilayer dual-mode resonator implementation achieves a footprint reduction while preserving the characteristics of the microstrip dual-mode resonator.

The miniaturized filter (MultiBPF-1B) is designed for the centre frequency of 1.6 GHz and fractional bandwidth (FBW) of 5.53%. The proposed miniaturized multilayer bandpass filter (MultiBPF-1B) is shown in Fig. 4 and the dimensions are presented in Table 2.

The comparison of simulated results of the microstrip filter with dual-mode resonator and its multilayer miniaturization is shown in Fig. 5. The results are in good agreement. The proposed filter miniaturization is intended

for compact implementations of microwave devices, resulting in footprint reduction around 50%.

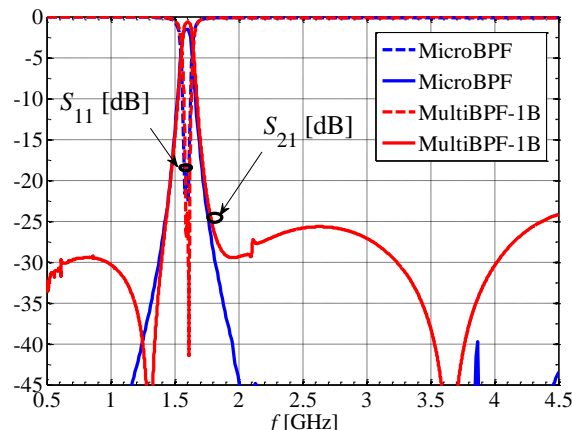


Fig. 5. Comparison of S-parameters, obtained by simulation, for MicroBPF (Fig. 1a) and MultiBPF-1B filters (Fig. 4)

4. Dual-band bandpass filter design

We present a novel realization of the multilayer filter with two pass bands. The proposed dual-band filter is realized by using a multilayer dual-mode resonator for each band. The multilayer dual-mode resonator is obtained by folding the microstrip dual-mode resonator to reduce the footprint (see Fig. 2).

Sketch of the conductors of the proposed dual-bend filter and the 3D EM model are shown in Fig. 6.

The positions of the resonators on the substrate and their orientation are chosen in such a way to practically eliminate the unwanted mutual coupling. Consequently, the resonators can be independently tuned for each pass band, i.e. centre frequency and bandwidth can be independently controlled.

The dual-band bandpass filter (MultiBPF-2B) is designed for the centre frequencies of 1.6 GHz (I-Band) and 3.5 GHz (II-Band), with fractional bandwidths (FBW) of 6.8% (I-Band) and 7.14% (II-Band). These bands are used for GPS navigation and WiMAX access, respectively.

First, we design two bandpass filters for I-Band (MultiBPF-1B-I) and II-Band (MultiBPF-1B-II). Subsequently, the dual-band bandpass filter (MultiBPF-2B) is realized as a parallel connection of two bandpass filters. The bands of MultiBPF-2B are annotated as MultiBPF-2B-I (I-Band) and MultiBPF-2B-II (II-Band). The appropriate dimensions obtained from the 3D EM model are given in Table 3.

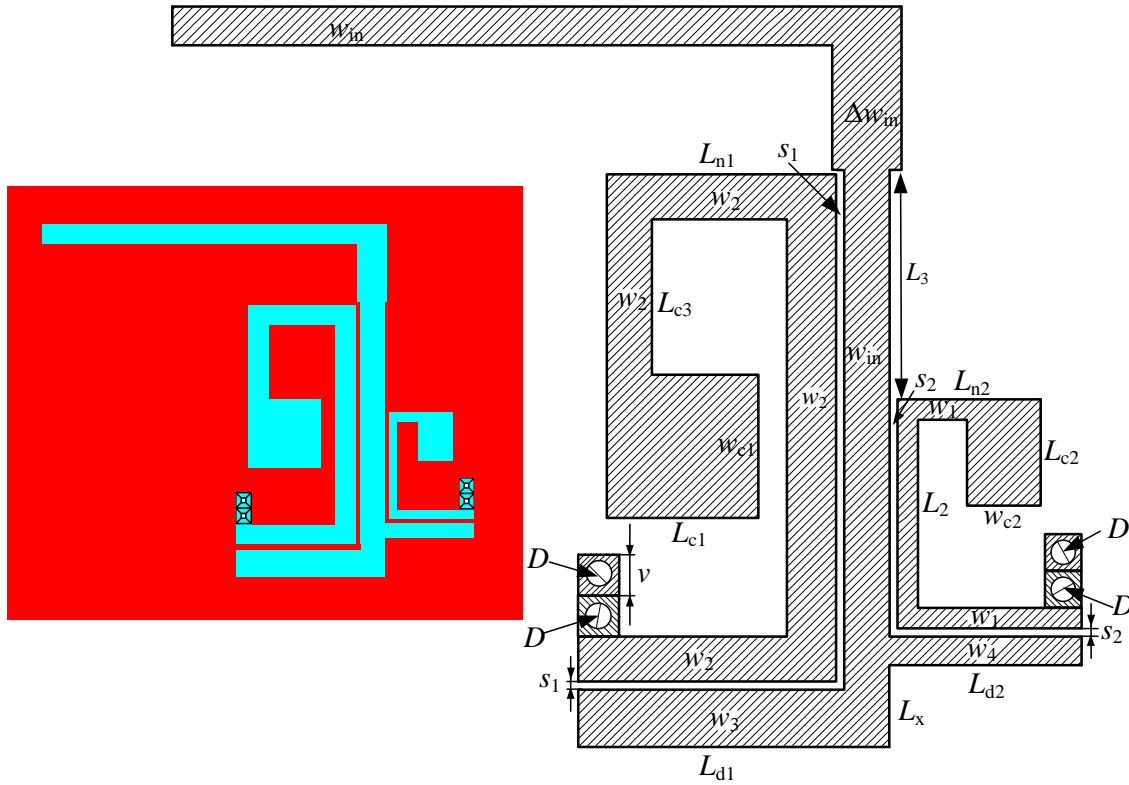


Fig. 6. 3D EM model and sketch of the multilayer dual-band bandpass filter

Table 3. 3D EM model parameters of the filter shown in Fig 6. All dimensions are in mm

MultiBPF-2B-I	w_2	1.1	MultiBPF-2B-II	w_1	0.5
	s_1	0.13		s_2	0.11
	L_{d1}	6.28		L_{d2}	4.8
	L_{n1}	4.6		L_{n2}	2.8
	w_{c1}	2.7		w_{c2}	1.45
	L_{c1}	2.85		L_{c2}	1.72
	L_{c3}	3.8		L_2	3.25
	w_3	1.4		w_4	0.7
Other dimensions					
L_x	2.02	D	0.5	w_{in}	1.1
L_3	5.55	v	1.0	Δw_{in}	1.46

Table 4. The comparison of FBW of the multilayer single band filters and dual-band bandpass filter

Filter type	f_0 [GHz]	FBW [MHz]
MultiBPF-1B-I	1.6	90
MultiBPF-1B-II	3.5	260
MultiBPF-2B-I	1.6	89
MultiBPF-2B-II	3.5	260

Table 4 shows the comparison of the frequency responses of the multilayer single band bandpass filters (MultiBPF-1B-I and MultiBPF-1B-II) and the dual-band bandpass filter (MultiBPF-2B) for the centre frequencies of 1.6 GHz and 3.5 GHz.

Good agreement between the filter responses in pass bands can be noted in Fig. 7. MultiBPF-2B occupies a rectangle of $0.09 \lambda_g \times 0.09 \lambda_g$ (11.08 mm x 11.1 mm)

excluding the feed lines and guard zone, and 11.08 x 12.63mm ($0.09 \lambda_g \times 0.104 \lambda_g$) including the feed lines. λ_g is the guided wavelength of a 50 Ω line on the substrate for the centre frequency of the first passband (1.6 GHz). The proposed implementation of the filter in Fig. 6 enables the reduction of the footprint. For each of the resonators the reduction is around 50% compared to the microstrip implementation.

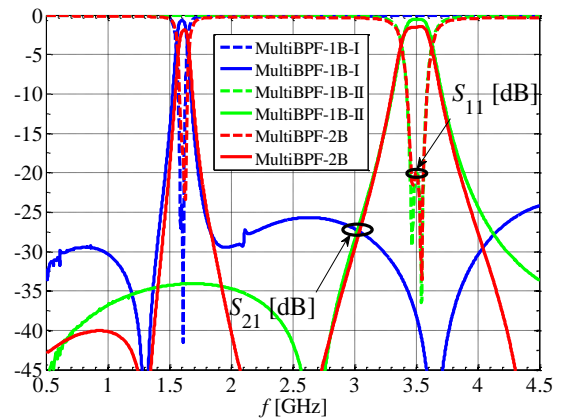


Fig. 7. Comparison of frequency responses of MultiBPF-2B and single band filters MultiBPF-1B-I and MultiBPF-1B-II

5. Circuit model of dual-band bandpass filter

The filter implementation using multilayer resonators is very flexible, but the 3D EM simulation is time consuming and requires extensive computer resources. In

this paper, one of our objectives is to reduce the simulation time. We are using the concept of the circuit model as a primary tool to analyze and design a filter. Using the diakoptic approach, the 3D filter structure is decomposed into domains and each of them is modelled by a microwave network.

efficiently used to identify the key filter parameters, which predominantly affect the filter characteristics. These key parameters can be effectively used to fine-tune the filter performance and meet the specifications. Using circuit models, the desired bandpass filters are designed. After fine tuning, these filters are analyzed by the 3D EM solvers.

Table 5. Circuit model parameters of the filter shown in Fig. 8. All dimensions are in mm

MultiBPF-2B-I	w_2	1.1	MultiBPF-2B-II	w_1	0.5
	s_1	0.14		s_2	0.09
	L_{d1}	6.5		L_{d2}	4.4
	L_{n1}	4.6		L_{n2}	2.8
	w_{c1}	2.7		w_{c2}	1.45
	L_{c1}	2.85		L_{c2}	1.72
	L_{c3}	3.8		L_2	3.25
w_3	1.4	w_4	0.7	Other dimensions	
L_x	1.42	D	0.5	w_{in}	1.1
L_3	5.55	w_{gnd1}	7.5	w_{gnd2}	2.5

Compared to the 3D EM simulators, the circuit-level simulators analyze the filter almost instantaneously. Therefore, the repeated circuit simulations can be

The proposed circuit model of the multilayer filter (shown in Fig. 6) is presented in Fig. 8.

The dimensions of the circuit model are shown in Table 5. The circuit-level simulations are performed by NI AWR Microwave Office [20].

The filter’s frequency response obtained by WIPL-D is compared to the simulation results generated by NI AWR Microwave Office and there is a good agreement as shown in Fig. 9. However, dimensions of the distributed circuit elements are slightly modified to match desired filter response obtained by the 3D EM simulation.

Table 6 shows the comparison of the filter characteristics for the 3D EM model with the equivalent circuit model of MultiBPF-1B-I, MultiBPF-1B-II and MultiBPF-2B. There is a relatively good agreement of the obtained results, thus the proposed circuit can be adopted as the relevant representation of the considered dual-band bandpass filter.

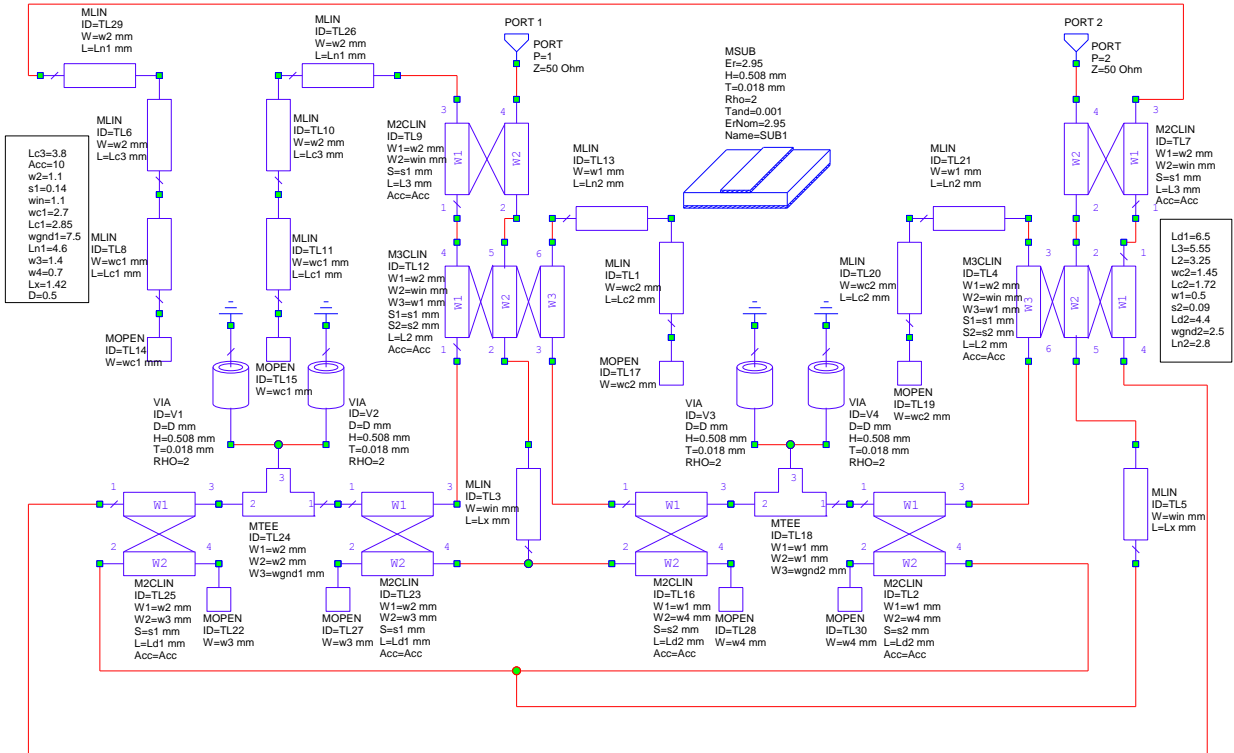


Fig. 8. Circuit model of MultiBPF-2B, shown in Fig. 6

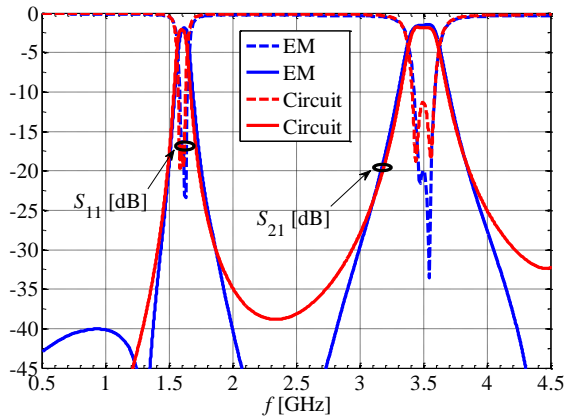


Fig. 9. The frequency response of MultiBPF-2B: 3D EM simulation and circuit-level simulation

Table 6. Comparison of the filter characteristics of the 3D EM model and the equivalent circuit model of MultiBPF-1B-I, MultiBPF-1B-II and MultiBPF-2B

	f_0 [GHz]	MWO		WIPL-D	
		S_{21} [dB]	B [MHz]	S_{21} [dB]	B [MHz]
Multi 1B	1.6	-1.9	90	-0.6	90
	3.5	-1.3	245	-1.2	260
Multi 2B	1.6	-1.9	90	-1.8	89
	3.5	-1.8	244	-1.52	260

6. Experimental verification

In order to validate the proposed design of the dual-band bandpass filter, the filter is fabricated and measured. The filter is implemented on laminate TLE-95-0200-CH/CH, with: $\epsilon_r = 2.95$, $\tan\delta = 0.001$, $h = 0.508$ mm, $t = 18$ μm .

The picture of the fabricated filter is shown in Fig. 10. Agreement can be observed between the measured and simulated responses in Fig. 11. Measured filter (3 dB) bandwidths are 90 MHz (I-band) and 266 MHz (II-band). The filter insertion losses are 1.85 dB (I-band) and 1.31 dB (II-band). The measured centre frequencies are 1.62 GHz

(I-band) and 3.5 GHz (II-band). The fabricated filter has a footprint of $0.09 \lambda_g \times 0.09 \lambda_g$.

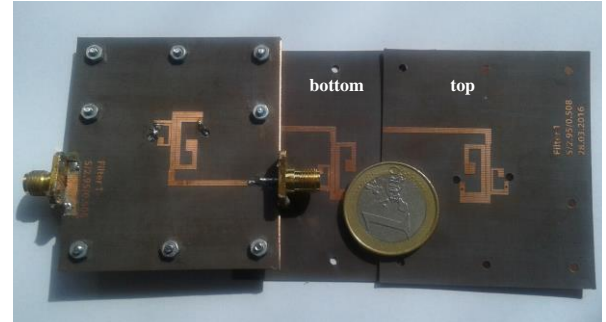


Fig. 10. Photograph of the fabricated dual-band bandpass filter

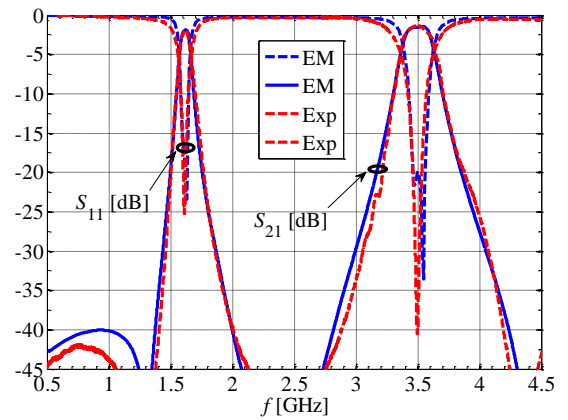


Fig. 11. Comparison of the frequency response of the 3D EM simulation and the measured response of the fabricated dual-band bandpass filter

In Table 7, we compare reported filters with our filter implementation. Our implementation exhibits a compact filter size in multilayer technology and very good results regarding the filter size reduction. The proposed filter is among the best achieved results (the smallest footprint) compared to other designs which use dual-mode resonators as in [11] ($0.22 \lambda_g \times 0.22 \lambda_g$), [17] ($0.25 \lambda_g \times 0.25 \lambda_g$), [21] ($0.24 \lambda_g \times 0.18 \lambda_g$), and in [22] ($0.17 \lambda_g \times 0.21 \lambda_g$).

Table 7. Comparison of our filter with reported implementations (f_0 - centre frequency, FBW - fractional bandwidth, IL - insertion loss)

Ref. No	I Band			II Band			Circuit size
	f_0 [GHz]	FBW [MHz]	IL [dB]	f_0 [GHz]	FBW [MHz]	IL [dB]	
[3] II filter	2.08	457	1.1	3.89	397	2.7	$1.347 \lambda_g \times 0.42 \lambda_g$
[11] filter C	1.794	119	1.38	2.825	140	2.1	$0.22 \lambda_g \times 0.22 \lambda_g$
[17] filter I	1.4	140	0.9	2.15	71	1.9	$0.25 \lambda_g \times 0.25 \lambda_g$
[14]	2.45	146	1.45	3.55	279	1.3	$0.43 \lambda_g \times 0.43 \lambda_g$
[9]	2.4	197	1.6	5.2	210	2.5	$0.74 \lambda_g \times 0.18 \lambda_g$
[21]	2.12	324	0.92	3.91	215	2.11	$0.24 \lambda_g \times 0.18 \lambda_g$
[22]	1.84	350	0.43	2.65	205	0.65	$0.17 \lambda_g \times 0.21 \lambda_g$
This work	1.62	90	1.85	3.5	266	1.31	$0.09 \lambda_g \times 0.09 \lambda_g$

7. Conclusions

In this paper, a novel design of a microwave filter using a dual-mode resonator has been presented. The filter has been realized in multilayer technology. The structure has consisted of two dielectric layers separated by the ground plane. The halves of the resonator have been printed on the outer sides of the two dielectric layers. The proposed filter realization has been intended for the compact implementations of microwave devices.

The dual-band filter has been implemented as a parallel connection of two bandpass filters. In addition, the resonators in the dual-band filter could be independently tuned for each pass band, i.e. the centre frequency and the bandwidth could be independently controlled.

The 3D EM modelling of the proposed filters has been performed by WIPL-D Pro EM Solver. In order to reduce the time needed for demanding 3D EM analyses, we have proposed the equivalent circuit models for faster filter analysis and design. The 3D filter structure has been decomposed into domains and each of them has been modelled by a microwave network.

The design methodology and experimental results have been presented. The dual-band bandpass filter has been fabricated on laminate TLE-95-0200-CH/CH. The measured results, circuit-level simulation and three-dimensional electromagnetic simulation were in good agreement. The dual-band bandpass filter has achieved a very small footprint due to the multilayer implementation ($0.09 \lambda_g \times 0.09 \lambda_g$).

The response of the proposed dual-band bandpass filter has been compared to the responses of the reported multilayer filters. Our filter achieved the smallest footprint compared to the similar approaches which use dual-mode resonators.

Acknowledgements

This work was supported by the Ministry of Education, Science and Technological Development of the Republic of Serbia under Grant TR-32005.

References

- [1] J.-S. Hong, "Microstrip Filters for RF/Microwave Applications", John Wiley & Sons, Hoboken, NJ, USA, 2nd edition, (2011).
- [2] F. J. Cervera, J. Hong, *IEEE T. Microw. Theory* **62**(11), 2618 (2014).
- [3] R. Gómez-García, M. Sánchez-Renedo, *IEEE T. Microw. Theory* **58**(12), 3760 (2010).
- [4] J. Lim, M. Nam, H. Choi, J. Lee, In *Proc. of the Asia Pacific Microwave Conf.*, Yokohama, Japan, 2010, p. 1114.
- [5] A. Görür, C. Karpuz, M. Akpınar, *IEEE Microw. Wirel. Co.* **13**(9), 385 (2003).
- [6] J. Bonache, I. Gil, J. García-García, F. Martín, *J. Comput. Electron.* **5**(2), 193 (2006).
- [7] R. R. Mansour, S. Ye, S. F. Peik, V. Dokas, B. Fitzpatrick, *IEEE T. Microw. Theory* **48**(12), 2476 (2000).
- [8] J.-S. Hong, M. J. Lancaster, *IEEE T. Microw. Theory* **47**(9), 1848 (1999).
- [9] S. Lee, Y. Lee, *IEEE Microw. Wirel. Co.* **20**(1) (2010).
- [10] M. Potrebić, D. V. Tošić, *Optoelectron. Adv. Mat.* **6**(3-4), 441 (2012).
- [11] A. K. Görür, C. Karpuz, In *Proc. of the 41st European Microw. Conf.*, Manchester, UK, 2011, p. 468.
- [12] A. Görür, C. Karpuz, In *Proc. of IEEE MTT-S International Microw. Symp.*, Honolulu, Hawaii, 2007, p. 905.
- [13] C. Zhou, Y. Guo, S. Yan, In *Proc. of the Asia Pacific Microw. Conf.*, Melbourne, Australia, 2011, p. 1278.
- [14] V. Radonić, V. Crnojević-Bengin, A. Baskakova, I. Vendik, In *Proc. of 2014 Mediterranean in Microw. Symp. (MMS 2014)*, Marrakech, Morocco, 2014, p. 1.
- [15] H.-S. Peng, Y.-C. Chiang, *IEEE Microw. Wirel. Co.* **25**(1), 7 (2015).
- [16] W. Feng, X. Gao, W. Che, Q. Xue, *IEEE Microw. Wirel. Co.* **25**(5), 295 (2015).
- [17] X. Y. Zhang, Q. Xue, *IEEE T. Microw. Theory* **55**(10), 2183 (2007).
- [18] WIPL-D Pro 10.0, 3D Electromagnetic Solver, WIPL-D d.o.o., Belgrade, Serbia. [online] <http://www.wipl-d.com/>.
- [19] A. Plazinić, M. Potrebić, D. V. Tošić, In *Proc. of the 12th Internat. Conf. on Applied Electromag.* (IIEC 2015), Niš, Serbia, 2015, p. 81.
- [20] Microwave Office, National Instruments AWR, El Segundo, CA, USA. [online] <http://www.awrcorp.com/>.
- [21] H. Chen, K. Chen, X. Chen, J. Electromagnet. Wave. **30**(15), 1964 (2016).
- [22] S. Yang, L. Lin, J. Chen, K. Deng, C.-H. Liang, *Electron. Lett.* **50**(8), 611 (2014).

*Corresponding author: milka_potrebic@etf.rs